Magnesium Technology 2013
Edited by: Norbert Hort, Suveen N. Mathaudhu, Neale R. Neelameggham, and Martyn Alderman
TMS (The Minerals, Metals & Materials Society), 2013

AGING BEHAVIOR AND MICROSTRUCTURAL EVOLUTION IN MG-3ND-0.2ZN-0.5ZR ALLOY

Amirreza Sanaty Zadeh[1], Xiangyu Xia[1], Alan A. Luo[2], Joseph E. Jakes[3], Donald S. Stone[1]

[1]Materials Science and Engineering Department; University of Wisconsin, Madison, WI, 53706
[2] Chemical and Materials Systems Laboratory; General Motors Research and Development Center; Warren, MI, 48090
[3]Performance Enhanced Biopolymers, Forest Products Laboratory, Madison, WI 53726

Keywords: Mg-Zn-Nd; Precipitation hardening; Transmission Electron Microscopy

Abstract

The aging behavior and microstructure evolution of Mg-0.2Zn-3Nd-0.5Zr alloy were studied in this paper. Transmission Electron Microscopy investigations showed four sets of precipitates formed during aging. These precipitates are β" which forms on prismatic planes during early stages of precipitation, γ' which forms on basal plane, and β' which forms on prismatic and pyramidal planes. In addition, some unknown precipitates in the form of dark spots were detected in 8 hours aged sample. The results from nanoindentation showed an activation volume in the range 80-100 b^3 that is consistent with prismatic glide as the rate controlling mechanism in the system. Furthermore, a small amount of dislocation climb along with dynamic recovery occur at room temperature upon deformation in this system.

Introduction

There has been significant attention paid to magnesium and its alloys due to their high specific strength. The application of magnesium products are in aerospace and automotive industries for reducing energy consumption. However, poor ductility of magnesium due to its structure (HCP) limits its applications. Modification of texture is reported to improve the ductility of magnesium alloys greatly [1-3]. This is done by alloying magnesium with rare-earth elements such as Ce, Nd, and Gd [4, 5]. It has also been reported that the addition of rare earth elements has a significant effect on creep resistance of Mg alloys both at room and elevated temperatures. Among the rare earth elements, neodymium (Nd) has relatively high solid solubility at the eutectic point and is more suitable for texture randomization and age hardening. Also, Nd plays an important role in precipitation strengthening of magnesium alloys. The strengthening can be enhanced by controlled addition of third element such as zinc. It has been reported that small addition of Zn to Mg–Nd binary system causes an increase in the precipitation hardening effect and the mechanical properties. It should be mentioned that the amount of zinc seems to change the sequence and nature of precipitation. It has been reported that higher amounts of Zn (>1 wt.%) reduces the precipitation hardening effect by restricting the precipitation of Mg-Nd phase. Therefore, combining the effect of solid solution strengthening from zinc as well as precipitation strengthening form Nd would result in improved mechanical properties. These effects have been reported in previous works [6-8].

The sequence of precipitation in binary Mg-Nd alloys is somehow different from ternary Mg-Zn-Nd alloys. In Mg-Nd alloys, the sequence is reported to be: supersaturated solution –G.P. zones- β"- β'- β, which was modified later with addition of another intermediate phase β_1 (fcc) forming during β' precipitation [9]. In Mg-2.8wt%Nd-1.3wt%Zn alloy, the sequence is reported to be supersaturated solution- low-temperature reaction- γ" - γ' - γ [7, 8]. The nature of low-temperature reaction has not been fully elucidated but it is believed to be –G.P. zones. The results showed that the ratio of Nd/Zn affects the sequence and kinetics of precipitation, which further affect the mechanical properties.

Due to limited research on the precipitation and the nature of precipitates in Mg-Zn-Nd system, there is not a comprehensive understanding of precipitation in this system. In addition, although there are reports on the characterization and mechanical properties of this alloy [10-19], there is not a detailed study on the deformation mechanisms involved at room temperature in this system. Therefore, in this research, it is aimed to further investigate the precipitation of metastable phases and deformation mechanisms at room temperature in this alloy. For this purpose, Transmission Electron microscopy and nanoindentation including Broadband Nanoindentation Creep (BNC) [20, 21] were used to characterize the microstructure and generate mechanical properties data.

Experimental

The as-cast ingot of Mg-3Nd-0.2Zn-0.5Zr alloy was prepared by mixing and casting of pure magnesium, zinc, zirconium, and Mg-20Nd master alloy ingots in an electric furnace and under protection of SF_6/CO_2. Cubic samples of $1\times1\times0.5$ cm^3 were cut from the ingot, polished, and cleaned in alcohol using ultrasonic cleaning. Samples then were wrapped in Ta foil and encapsulated in glass ampules under He atmosphere. Heat treatment of the samples was done using a horizontal tube furnace. Samples were first solution-treated at 540 °C for 4 hours followed by quenching in water at 20 °C. After solid solution treatment, the samples were placed in fridge for 24 hours. The aging of the samples was done using the same sample preparation method but at 200 °C for different aging times. For hardness measurements, Scanning Electron Microscope (SEM), and nanoindentation tests, samples were prepared using Allied Multiprep machine and diamond lapping films (15 μm, 3 μm, 1 μm, and 0.1 μm). Hardness tests were performed using a Wilson Tukon 1102/1202 micro-hardness tester (Wilson Hardness, Norwood, MA). SEM and EDS analyses were done using a LEO 1530 equipped with an EDS detector. Nanoindentation tests were conducted using a Hysitron TI 900 TriboIndenter (Hysitron, Minneapolis, MN). Transmission Electron Microscopy (TEM) studies were performed on a high resolution Philips CM200. The wedge TEM samples were prepared on an Allied Multiprep machine using diamond lapping films with different grid sizes from 15 μm down to 0.1 μm. The wedge samples were further thinned using Fischione 1010 ion milling instrument.

Results and Discussion

Microstructure

Fig. 1 shows the results of age hardening experiments of NZ30K alloy. Also the hardness values are compared with the results in previous publications [7, 11, 13]. As can bee seen, the peak hardness in this work occurs at around 8 hours aging time. This agrees well with Ma et al [7], although Xingwei et al [11] and Ding et al [13] showed peak hardness at about 12 and 16 hours, respectively. It is noted that the maximum hardness in this work is about 10 HV higher than the values in the previous reports [7, 11, 13]. The reason can be attributed to the fact that the samples were pre-aged at 273 K for 24 hours in this study, which causes some pre-existing clusters in the solid solution samples to grow into critical nucleation sizes for precipitation. Another reason could be the different quenching conditions used. In previous reports, samples were quenched in hot water (~70 °C), while in this work the samples were quenched in cold water (20 °C), which results in faster quenching rate and higher vacancy concentration in the sample. These vacancies play significant role in precipitation, especially in early stages of precipitation and in the formation of G.P. zones [6, 8].

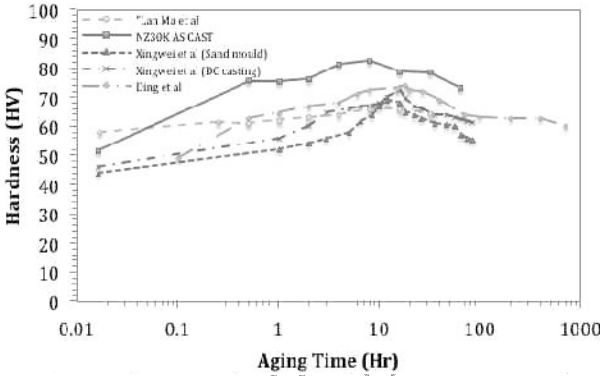

Fig. 1. Aging curve for NZ30K (Mg-3Nd-0.2Zn-0.5Zr).

Fig. 2 shows the XRD patterns obtained from selected aged samples. As can be seen, in the as cast sample, the microstructure is mainly composed of α Mg, $Mg_{12}Nd$ and $Mg_{41}Nd_5$. These phases are concentrated on grain boundaries, as shown in the elemental maps of the as-cast sample in Fig. 3.

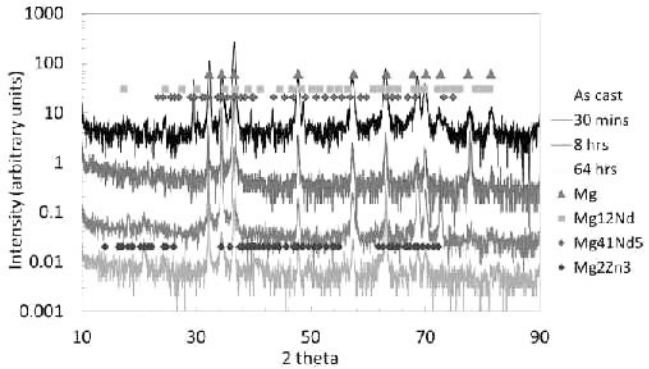

Fig. 2. XRD patterns of NZ30K samples aged at 200 200 °C for different length of time.

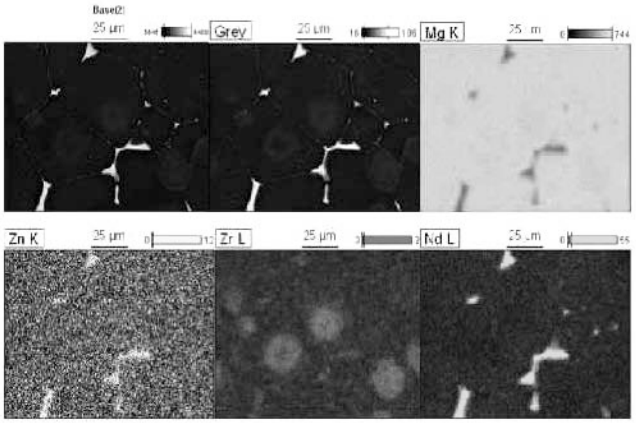

Fig. 3. EDS map of NZ30K as cast sample

Fig. 4 shows the elemental maps of the as-cast sample after solid solution treatment. The maps show no evidence of eutectic phase on grain boundaries indicating good dissolution of the eutectic phase during solution treatment. In addition, in some grains, a concentration of some small and large precipitates was observed. These precipitates, as confirmed by EDS, are zirconium concentrated phases, which form during the solidification of the ingot. Due to the fact that the formation of these precipitates occur at around 700 °C, the solution treatment does not affect these precipitates. No evidence of the presence of Zr could be detected on grain boundaries.

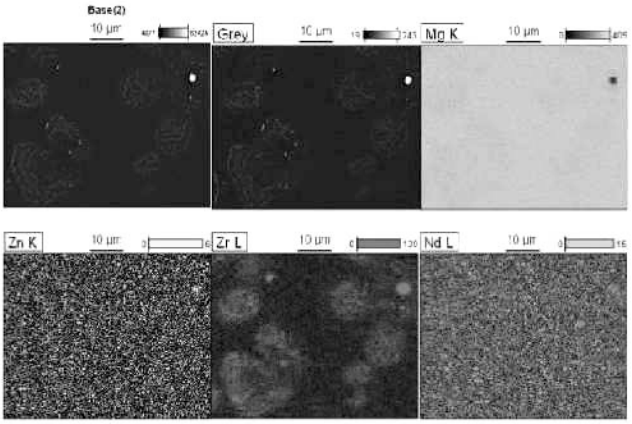

Fig. 4. EDS maps of NZ30K sample solid solution treated at 540°C

Also, the XRD patterns for aged samples at 200 °C for different times show that the peaks related to $Mg_{12}Nd$ and $Mg_{41}Nd_5$ phases are somewhat weak and absent in some cases. It should be pointed out that for the 8 hours aged sample some Mg_2Zn_3 peaks can be detected, which become stronger in 64 hours aged sample. The TEM micrograph taken from a grain boundary (see Fig. 5) confirms the appearance of these precipitates on grain boundaries after 8 hours aging. Precipitation of these phases has been observed in previous researches [10]. The existence of other intermediate phases could not be detected from the XRD patterns; therefore, TEM was employed to study these intermediate phases in the selected samples.

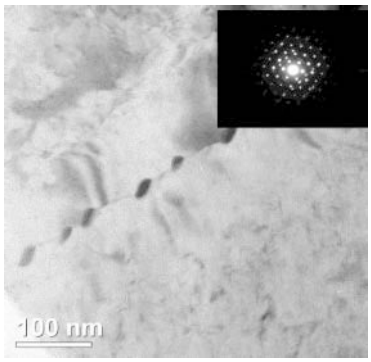

Fig. 5. Grain boundary precipitates in 8 hrs aged sample of NZ30K

An investigation on 30 minutes aged sample showed no apparent precipitation throughout the sample, instead, some coherent metastable and intermediate phases were observed precipitated randomly in some grains. Fig. 6 shows BF TEM micrographs of these precipitates in the 30 minutes aged sample. The beam is parallel to [11-20] direction. As can be seen, there are 3 sets of precipitates visible in these micrographs. In Fig. 6 a, there are two sets of precipitates on prismatic and basal planes. In Fig. 6 b, in addition to the first two sets, there are some unknown dark spots that do not have any clear orientation with the matrix.

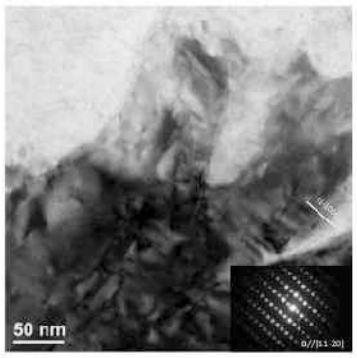

(a)

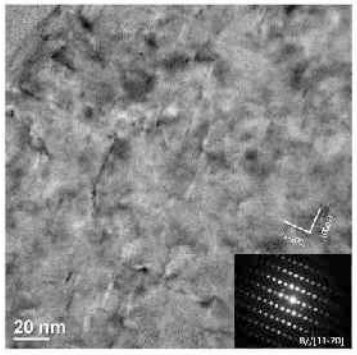

(b)

Fig. 6. – TEM micrographs showing coherent β″ precipitates on {1-100} prism planes, coherent γ′ precipitates on basal planes, and unknown dark spots. The beam is parallel to [11-20].

In the corresponding diffraction pattern, there are some extra spots which are at ½ 0 0 position. These spots were used for dark field imaging in order to study their origin. As can be seen in Fig. 7, these spots belong to sets of precipitates, which lie on {01-10} prism planes.

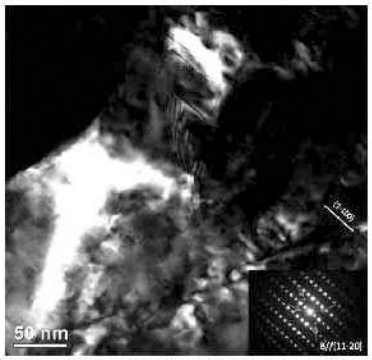

Fig. 7. DF image of the precipitates taken from extra spots in diffraction pattern. The beam is parallel to [11-20] direction.

Fig. 8 shows a high-resolution image of these precipitates. The precipitates are 5- 20 nm long and about 2-3 atomic layers thick with the aspect ratio of 20. According to Ref. 6, 7 and 21, these precipitates are likely either coherent G.P. zones or coherent metastable β″ which form in early stages of precipitation and on {01-10} or {11-20} prims planes. The small size of these precipitates does not allow us to perform a SAED from individual precipitates. The β″ precipitates have D019 structure with $a_{\beta''}=2a_{Mg}$ and $c_{\beta''}=c_{Mg}$. Since the structure of G.P. zones is reported to be disordered D019 structure in this system [22], it is still not clear to the authors whether these precipitates are G.P. zones or coherent β″. However, since in previous researches on G.P. zones, streaks in diffraction patterns are related to the existence of G. P. zones, these precipitates are designated as β″ due to the fact that no streaks could be detected in the corresponding diffraction pattern. With regard to the fact that aging was performed at a short time, this could indicate that the formation of G.P. zones in this system at 200 °C is either not feasible or too fast and cannot be detected. Further studies are underway, using DSC and resistivity measurements, to investigate this matter in Mg-Zn-Nd system.

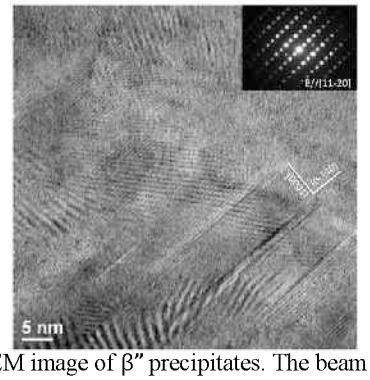

Fig. 8. HRTEM image of β″ precipitates. The beam is parallel to [11-20] direction.

Because the second set of precipitates are on basal planes and there are no additional reflections in the SAED pattern, acquired from the α-Mg matrix containing both sets of precipitates, these

precipitates are designated to be coherent γ′. According to Nie et al [23], the structure of γ' is disordered hexagonal with $a_{\gamma'}$ = 0.321 nm and $c_{\gamma'}$ = 0.781 nm. These precipitates are Mg-Zn rich precipitates, which further increase the hardness of the alloy by pinning dislocations on basal planes. The combination of these two sets of precipitates, which act as barriers to dislocation motion on basal and prismatic planes, results in further increase in the hardness of the alloy. The ratio of Nd/Zn is the factor controlling the formation of precipitates and therefore changes the precipitation nature.

Fig. 9 shows BF images from the 8 hours aged sample. As can be seen the density of precipitates in this sample is higher and the precipitates are uniformly distributed within the grains. The precipitates are on {01-10} prism planes and are 50-80 nm long and 5-7 nm thick. These precipitates are designated as β′ with base centered orthorhombic structure and lattice parameters of $a_{\beta'}$ = 0.64 nm, $b_{\beta'}$ = 2.22 nm, $c_{\beta'}$ = 0.64nm. HRTEM studies of this region, Fig. 10, reveal that beside prism plane precipitates, there are two other kinds of precipitates existing in the image taken. The first one is the presence of unknown precipitates in the form of dark spots, which do not have specific orientation with the matrix and are uniformly distributed in the grains. The second set of precipitates is the ones lying on {0-111} pyramidal planes. This orientation with the matrix has not been observed in this system before. However, this orientation has been reported for Mg-Sn-Zn system [24]. The volume fraction of these precipitates was decreased by addition of Ce into the system [24]. The nature of the precipitates is not still clear. However, since the morphology and dimensions of these precipitates are similar to β′ and these precipitates were just observed in the 8 hours aged sample, these precipitates are designated as β′. Also, the diffraction pattern taken from the region containing these precipitates did not show any additional reflection. The existence of the new set of precipitates on pyramidal planes can further pin the dislocation movement, which results in an increase in hardness, as seen earlier in Fig. 1 for the 8 hours aged sample.

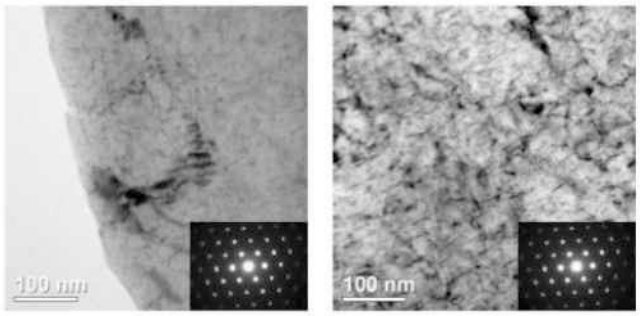

Fig. 9. BF images of NZ30K aged for 8 hours at 200 °C. The beam is parallel to [1-21-3] direction.

Mechanical Properties

In order to study the mechanical properties of the alloy, nanoindentation and Broadband Nanoindentation Creep (BNC) [20, 21] were performed on 4 different samples of solid solution treated, under-aged (30 minutes aging time), peak-aged (8 hours aging time), and over-aged (64 hours ageing time) samples.

The results are shown in Fig. 11 in the form of hardness as a function of indentation load. As can be seen, the data shows an indentation size effect (a decrease in the hardness with an increase in the load). The results of micro-hardness are also added to the graph for comparison. The hardness values are not completely consistent with the values obtained from microhardness for the 8 hours aged sample. This can be attributed to the fact that the nanoindentation results are more sensitive to thermo-mechanical treatment and surface preparation than the microhardness data, causing the observed discrepancy. For both methods, the over-aged sample has the lowest hardness value.

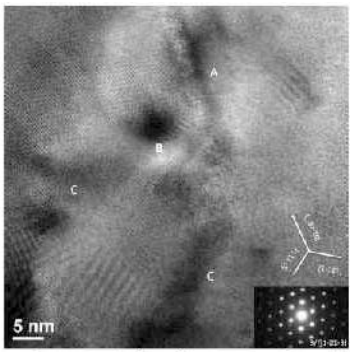

Fig. 10. HRTEM image of the 8hours aged sample. The beam is parallel to [1-21-3]. There are 3 different type of precipitates visible in this image which are marked as: a) prism b) unknown precipitates in the form of a dark spot, and C) pyramidal precipitates.

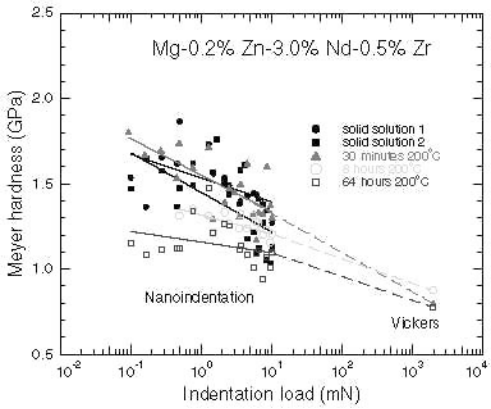

Fig. 11. Hardness (GPa) vs. indentation load (mN) for Mg-0.2Zn-3Nd-0.5Zr alloy. The microhardness values added to the graph for comparison.

The BNC experiments were designed to study the mechanisms involved in the deformation of different samples. The procedure was such that the indenter was loaded into the specimen as rapidly as possible and then was held for as long as possible (until significant drift). The data was corrected for electronic delay during rapid loading. A schematic of load-depth curve (with and without instrumental corrections is shown in Fig. 12 [20].

Fig. 13 shows BNC results in the form of hardness (GPa) vs. strain rate (1/s). The strain rate is extended to 5 orders of magnitude. For all the samples, the hardness tends to increase as the strain rate increases. Also further inspection of the curves reveals that for all the curves, there is a slight downward curvature. This phenomenon is probably caused by dynamic

recovery during deformation [25, 26] and a small amount of dislocation climb at room temperature [27]. In addition activation volumes calculated from the BNC data range from 80-100 b^3, which is consistent with prismatic glide as the rate-controlling mechanism in this system.

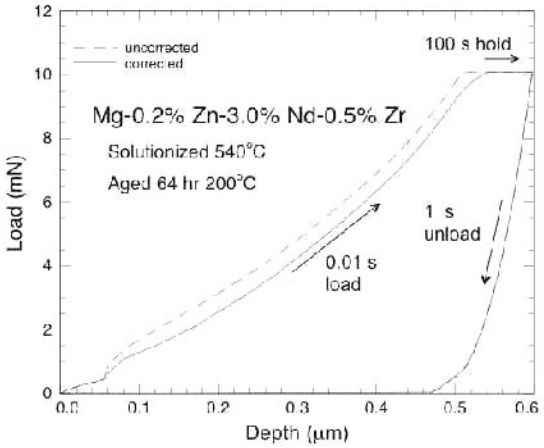

Fig. 12. Load-depth trace from BNC performed on the Mg-0.2Zn-3Nd-0.5Zr

It should be pointed out that the shift in the position of the curves with respect to each other is due to the fact that precipitation hardening mechanism introduces an athermal component (i.e. constant, independent of the strain rate) that contributes to the flow stress of the aged alloy and results in shifting the curves.

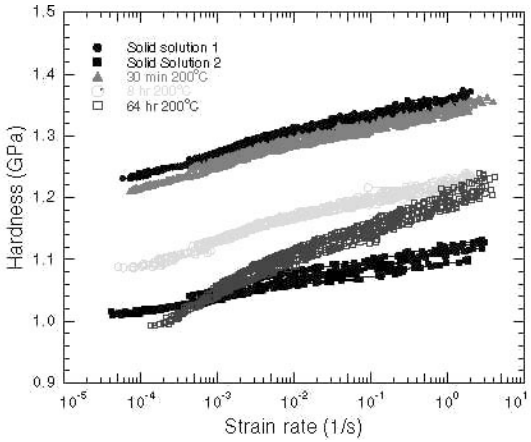

Fig. 13. Hardness vs. Strain Rate curve for the tested samples at different aging times.

Conclusion

1. Four sets of precipitates formed during aging of Mg-0.2Zn-3Nd-0.5Zr alloy at 200 °C which are β" , β', γ' and an dark spots.

2. β" precipitates form on prismatic planes during early stages of precipitation, along with γ' precipitates which form on basal planes. β' precipitates form at higher aging times and precipitate on both prismatic and pyramidal planes. In addition, some unknown precipitates in the form of dark spots were detected at higher aging times. These precipitates had no specific orientation with the matrix.

3. BNC experiments showed an activation volume in the range 80-100 b^3 that is consistent with prismatic glide as the rate controlling mechanism in the system. Furthermore, a small amount of dislocation climb along with dynamic recovery occur at room temperature upon deformation in this system.

Acknowledgement

This work was fully supported by National Science Foundation, DMR GOALI Program, Grant No. 1005762.

References

1. N. Stanford, M. Barnett, "Effect of composition on the texture and deformation behavior of wrought Mg alloys' Scripta mater. 58 (2008) 179-182.

2. R. Gehrmann, M. M. Frommert, G. Gottstein, "Texture effects on plastic deformation of magnesium" J. Mater. Sci. Eng. A 395 (2005) 338-349.

3. A. Sanaty-Zadeh, P. K. Rohatgi, "Comparison between current models for the strength of particulate-reinforced metal matrix nanocomposites with emphasis on consideration of Hall-Petch effect" J. Mater. Sci. Eng. A 531 (2012) 112-118.

4. K. Hantzsche, J. Bohlen, J. Wendt, K. Kainer, S. Yi, D. Letzig, "Effect of rare earth additions on microstructure and texture development of magnesium alloy sheets" Scripta Mater. 63 (2010) 725-730.

5. R. K. Mishra, A. K. Gupta, P. R. Rao, A. K. Sachdev, A. Kumar, A. Luo, "Influence of cerium on the texture and and ductility of magnesium extrusions" Scripta Mater. 59 (2008) 562-565.

6. T. J. Pike, B. Noble, "The formation and structure of precipitates in a dilute magnesium-neodymium alloy" J. the Less-Common Met. 30 (1973) 63-74.

7. L. Ma, R. K. Mishra, M. P. Balogh, L. Peng, A. A. Luo, A. K. Sachdev, W. Ding, "Effect of Zn on the microstructure evolution of extruded Mg-3Nd(-Zn)-Zr (wt.%) alloys" J. Mater. Sci. Eng. A 543 (2012) 12-21.

8. P. A. Nuttall, T. J. Pike, B. Noble, "Metallography of Dilute Mg-Nd-Zn alloys" Metallography 13 (1980) 3-20.

9. K.Y. Zheng, J. Dong, X.Q. Zeng, W.J. Ding, "Precipitation and its effect on the mechanical properties of a cast M-Gd-Nd-Zr alloy" J. Mater. Sci. Eng. A 489 (2008) 44-54.

10. Zheng Xingwei, Dong Jie, Liu Wencai, Ding Wenjiang, "Microstructure and mechanical properties of NZ30K alloy by semi-continuous direct chill and sand mould casting processes" Res. Dev. 8 (2011) 41-46.

11. Xingwei Zheng, Alan A. Luo, Jie Dong, Anil K. Sachdev, Wenjiang Ding, " Plastic flow behavior of a high-strength magnesium alloy NZ30K" Mat. Sci. Eng. A 532 (2012) 616– 622.

12. Jun Dai, Jian Huang, Min Li, Zhuguo Li, Jie Dong, Yixiong Wu, "Effect of heat treatments on laser welded Mg-rare earth alloy NZ30K" Mat. Sci. Eng. A 529 (2011) 401– 405.

13. W.J. Ding, P.H. Fu, L.M. Peng, H.Y. Jiang, X. Q. Zeng, "Study on the microstructure and mechanical property of high strength Mg-Nd-Zn-Zr alloy" Mat. Sci. Forum 546-549 (2007) 433-436.

14. Xingwei Zheng, Jie Dong, Yazhen Xiang, Jianwei Chang, Fenghua Wang, Li Jin, Yingxin Wang, Wenjiang Ding, "Formability, mechanical and corrosive properties of Mg-Nd-Zn-Zr magnesium alloy seamless tubes" Mater. Des. 31 (2010) 1417–1422.

15. Wu Wen-Xiang, Jin Li, Dong Jie, Ding Wen-Jiang, "Prediction of flow stress of Mg-Nd-Zn-Zr alloy during hot compression" Trans. Nonferrous. Met. Soc. China 22 (2012) 1169−1175.

16. Ding Wenjiang, Li Daquan, Wang Qudong, Li Qiang, "Microstructure and mechanical properties of hot-rolled Mg-Zn-Nd-Zr alloys" Mater. Sci. Eng. A 483–484 (2008) 228–230.

17. Qiang Li, Qudong Wang, Yingxin Wang, Xiaoqin Zeng, Wenjiang Ding, "Effect of Nd and Y addition on microstructure and mechanical properties of as-cast Mg-Zn-Zr alloy" J. Alloys Comp. 427 (2007) 115–123.

18. Xiao Zhou, Haitao Zhou, Zhendong Zhang, Ruirui Liu, Libin Liu, "Tensile properties of Hot Extruded Mg-Zn-Nd-Y-Zr alloy at elevated temperatures" Adv. Mat. Res. 415-417 (2012) 1157-1163.

19. Yang Lin, Gao Xiao-dan, Lin Li, Zou Peng, Chen Li-jia, Liu Zheng, "Microstructural evolution of rolled Mg-5Zn-3Nd(-Zr) alloy" Trans. Nonferrous Met. Soc. China 20 (2010) s498-s502.

20. J. E. Jakes, R. S. Lakes, D. S. Stone Broadband nanoindentation of glassy polymers: Part II. Viscoplasticity J. Mater. Res. 27 (2012) 475-484.

21. J. B. Puthoff, J. E. Jakes, H. Cao, D. S. Stone, Investigation of thermally activated deformation in amorphous PMMA and Zr-Cu-Al bulk metallic glasses with broadband nanoindentation creep J. Mater. Res. 24 (2009) 1279-1290.

22. R. Wilson, C. J. Bettles, B. C. Muddle, J. F. Nie, "Precipitation hardening in Mg-3wt%Nd(-Zn) casting alloys" Mater. Sci. Forum 419-422 (2003) 267-272.

23. J. F. Nie, K. Oh-ishi, X. Gao, K. Hono, "Solute segregation and precipitation in a creep-resistant Mg-Gd-Zn alloy" Acta Mater. 56 (2008) 6061-6076.

24. C. Weili, P. S S, T. Weineng, Y. B S, K. B H, "Influence of rare earth on the microstructure and age hardening response of indirect-extruded Mg-5Sn-4Zn alloy, J. Rare Earths 28 (2010 785-789.

25. A. Couret and D. Caillard, "an in-situ study of prismatic glide in magnesium-I. The rate controlling mechanism" Acta Metall. 33 (1985) 1447-1454.

26. P. Lukáĉ and Z Trojanová, "Study of thermally activated dislocation motion in AJ51 and AE42 magnesium alloys" J. Phys.: Conference Series 240 (2010) 012-019

27. D. S. Stone, "Scaling laws in dislocation creep" Acta Met. et Mat. 39 (1991) 599-608.